Advanced Industrial and Engineering Polymer Research 1 (2018) 99–110

Contents lists available at ScienceDirect

Advanced Industrial and Engineering Polymer Research

journal homepage: http://www.keaipublishing.com/aiepr

Isothermal and non-isothermal crystallization kinetics of composites of poly(propylene) and MWCNTs

Nigel Coburn [a], Paula Douglas [b], Derya Kaya [c], Jaipal Gupta [d], Tony McNally [d, *]

[a] School of Mechanical & Aerospace Engineering, Queen's University Belfast, Belfast BT9 5AH, UK
[b] Polymer Processing Research Centre, Queen's University Belfast, Belfast BT9 5AH, UK
[c] Department of Civil Engineering, Dokuz Eylul University, 35160 Buca, Izmir, Turkey
[d] International Institute for Nanocomposites Manufacturing (IINM), WMG, University of Warwick, Coventry, CV4 7AL, UK

ARTICLE INFO

Article history:
Received 30 March 2018
Received in revised form
30 May 2018
Accepted 1 June 2018

Keywords:
Poly(propylene)
Carbon nanotubes
Composites
Crystallization kinetics
DSC

ABSTRACT

The isothermal and non-isothermal crystallization behaviour of composites of a poly(propylene) (PP) and multi-walled carbon nanotubes (MWCNTs) were investigated using Differential Scanning Calorimetry (DSC). An Avrami analysis was used to study the isothermal crystallization kinetics of unfilled PP and composites of PP with MWCNT loadings up to 2 (w/w). The value of the Avrami exponent (n) was greater than 2 for all samples, confirming the primary stage of crystal growth is a three-dimensional phenomenon. The activation energy (ΔE), determined using an Arrhenius type expression, for the isothermal crystallization of PP increased from 87 kJ for unfilled PP to 228 kJ on incorporation of 2 (w/w) MWCNTs to PP. An attempt was made to model the non-isothermal crystallization kinetics of composites of PP and MWCNTs using a range of mathematical models, including the Jeziorny extended Avrami equation, Ozawa equation, Cazé and Chuah average Avrami exponents, and a combined Avrami/Ozawa approach. The Jeziorny extended Avrami approach confirmed that the non-isothermal crystallization of MWCNT filled PP is clearly a two-stage process. Fitting of the Ozawa model was shown to be not valid and both the Cazé and Chuah average Avrami approaches were ineffective as neither took in to account the effects of secondary crystallization. Only the combined Avrami/Ozawa method successfully modelled the two-stage crystallization of composites of PP and MWCNTs. The activation energy (ΔE) for the non-isothermal crystallization of PP on addition of MWCNTs increased with increasing MWCNT content, up to as high as 726 kJ.

1. Introduction

The use of carbon nanotubes (CNTs) as functional 1D nanofillers for polymer matrices has received substantial attention with the targeted goal of producing advanced composite materials with multifunctional properties [1–3]. The exceptional intrinsic mechanical, thermal and electrical properties combined with a large effective surface area exhibited by CNTs can enhance polymer matrix performance when effective dispersion and distribution of the CNTs throughout the polymer matrix at minimal loadings is achieved [1,4]. Poly(propylene) (PP) is a versatile thermoplastic characterised by well-balanced physical and mechanical properties, low cost and density and, it is readily melt processable [1,4,5]. PP is a semi-crystalline polymer and the addition of (nano)fillers has shown to result in changes in crystalline content, crystal type, size and distribution [6]. PP is typically mixed with CNTs via melt blending in a twin screw extruder as it free of contamination from solvent residues and the number of CNT agglomerates can be minimised by way of application of appropriate shear stress [1]. During crystallisation, PP develops a partially ordered structure from the disordered melt phase. The trend towards shorter cycles times and faster cooling rates along with the addition of nucleating agents (CNTs) requires a better understanding of the crystallization kinetics of the composite and thus its final properties [7].

Addition of CNTs to PP has shown to enhance mechanical, electrical and thermal properties of the neat PP matrix [1] however, such modifications are not without changes in crystalline morphology of the polymer [4]. Due to their high aspect ratio, CNTs

* Corresponding author.
E-mail address: t.mcnally@warwick.ac.uk (T. McNally).

https://doi.org/10.1016/j.aiepr.2018.06.001

act as strong nucleating agents and significantly alter the polymer crystallization process [1]. The development of high performance composites requires a detailed understanding of the morphology, microstructure and crystallization behaviour post nanofiller addition in order to optimise the design of processing operations [4]. Changes in the properties of the polymer including, degree of crystallinity (X_c), affect the final properties of the composite and provides an insight into the interface between the filler and the polymer matrix [5]. Furthermore, the formation of trans-crystals and β-phase crystals can be explained by crystallisation kinetic behaviour [5,8]. There has been limited studies on the crystallization behaviour of PP reinforced with multi-walled carbon nanotubes (MWCNTs) under isothermal and non-isothermal conditions [4,9]. The addition of nucleating agents such as CNTs can be used to induce crystallisation at higher temperatures and thereby shorten processing cycle times. Crystallisation of PP is controlled by nucleation, crystal growth and the temperature differential with the environment. Crystallization rates can be increased by adding nucleating agents where heterogeneous nucleation occurs. The optical and mechanical properties of PP are strongly dependent on nucleation and crystal growth during cooling from the melt. Understanding the crystallization mechanisms with and without the presence of nucleating agents under dynamic conditions enables structure-property relationships to be developed which are key to producing composites with optimal properties [10]. Bulk crystallization of polymers is an important phenomenon and, understanding under-lying molecular processes, including nucleation, is important when trying to understand the resultant morphology changes upon the addition of MWCNTs. Schawe et al. described the nucleation efficiency of MWCNTs for an iPP using an acceleration factor, ε, i.e. simply the ratio of the crystallization time for the unfilled to the MWCNT filled polymer [11]. The authors showed that for α-polymorph formation, ε is a function of the number of nuclei per nanotube and the specific effect of the MWCNT on growth rate.

However, from a kinetics perspective and almost without exception workers use the Avrami or a modified version of the Avrami expression to describe the crystallization kinetics of CNT filled PP [12–16]. Avrami derived an equation for isothermal crystallization kinetics in terms of time dependence of the volume fraction of crystalline material X_v, accounting for the nucleation rate and crystal volume growth [17,18]. The Avrami model can be used to predict and quantify nucleation (homogeneous or heterogeneous) and crystal growth geometry by means of n, the Avrami exponent [19,20], but it is limited in describing the two-step crystallization of filled polymers.

Non-isothermal crystallization of semi-crystalline polymers from the melt closely matches that of industrially processed polymers. Typically, thermoplastics are extruded and injection moulded with cooling rates in excess of 500 K/min involving rapid quenching of polymers from the melt [10]. Ozawa extended the Avrami theory for non-isothermal events with a method of kinetic analysis of thermo-analytical data [17,21]. However, the theory has significant limitations, such as it is only valid for primary crystal growth before impingement [17]. Various theories and experimental techniques have been employed to determine kinetic parameters for non-isothermal crystallization of PP with nucleating agents including [10,22–24], Cazé et al. [19], Chuah et al. [17], Mo et al. [25], and Jeziorny et al. [26].

In this article, we report the isothermal and non-isothermal crystallization kinetics of composites of PP and a 1D nanofiller, MWCNTs, with loadings up to 2 wt% determined from differential scanning calorimetry (DSC) experiments. We test the validity of a range of mathematical models highlighted above to understand the crystallization behaviour of these composite materials.

2. Experimental

2.1. Materials and composite preparation

Poly(propylene) (PP) was kindly provided by Exxon Mobil Corporation, Europe; PP homopolymer 1364F4; MFI = 14 g/10 min and density = 0.9 g/cm^3. The multi-walled carbon nanotubes (MWCNTs) used were provided by Nanocyl S.A., Belgium, grade Nanocyl®7000 obtained in powder form with an average length and diameter of 1.5 μm and 9.5 nm, respectively. Composites of PP (powder) and MWCNTs at loadings of 0, 0.5, 1.25, 1.5, 1.75 and 2% (w/w) were prepared by initially pre-mixing using a Rondol High Speed Mixer at 2000 rpm for 30 s. These pre-mixed batches were then melt-mix in a Thermo Haake twin rotor batch mixer (Rheomix 600) at 200 °C and a rotor speed of 100 rpm for 10 min.

2.2. Differential scanning calorimetry

Isothermal and non-isothermal crystallization kinetic studies were carried out using a Perkin Elmer Diamond DSC and Perkin Elmer DSC 6 instruments, respectively, both controlled by Pyris software. For both studies all samples were weighed to 8 ± 0.5 mg using a Sartorias micro-balance. All samples were cut from pressed plaques of 0.5 mm thickness to maximize thermal conduction between the sample and pan. For the isothermal study, only samples of PP(h) (i.e. PP that has been melt processed and has the same thermal history as the composite materials, in contrast to PP(v), virgin unprocessed PP) and, composites of PP(h) and 1.25 wt% and 2 wt% MWCNTs were considered. The samples were heated from 30 °C to 200 °C at a rate of 20 K/min, held at 200 °C for 3 min (to eliminate any thermal history and ensure all previous crystalline structure was destroyed). The samples were then cooled at 200 K/min to a range of set crystallization temperatures spanning from 108 °C to 135 °C.The samples were then held at these preset temperatures for 30 min to encourage isothermal crystallization then cooled to 30 °C at 200 K/min. The thermograms as a function of time were recorded for each preset temperature. By way of example, the resultant thermograms for PP(h) and the composite with 1.25 wt% MWCNTs are shown in Figs. 1 and 2. For the non-isothermal study, all composites were analysed using the following temperature profile: heat from 30 °C to 200 °C, hold for 3 min at 200 °C; cool at different cooling rates of 5 K/min, 15 K/min, 25 K/min, 30 K/min and 40 K/min to 30 °C, then reheat to 200 °C at 20 K/min. The resultant thermograms were recorded for each cooling rate, see Figs. 3–7.

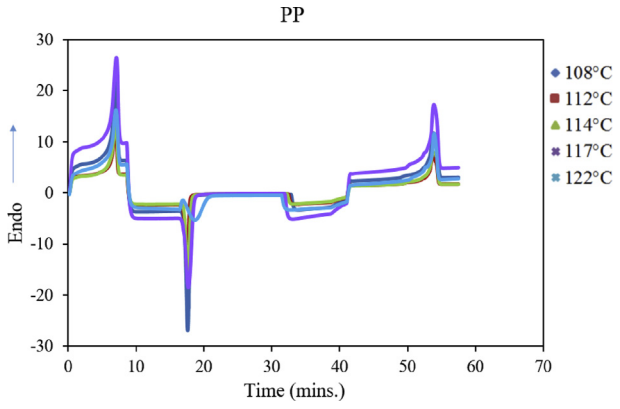

Fig. 1. DSC thermographs for PP recorded under isothermal conditions.

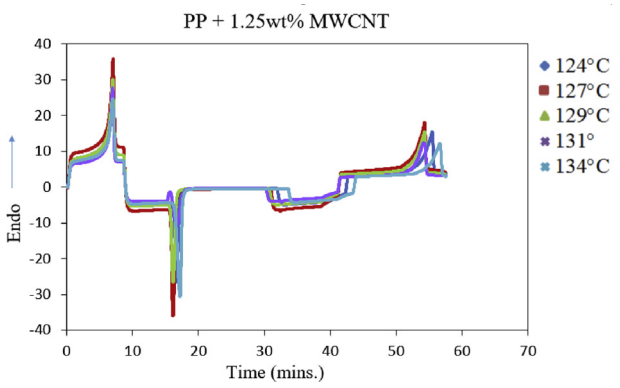

Fig. 2. DSC thermographs for a composite of PP and 1.25 wt% MWCNTs recorded under isothermal conditions.

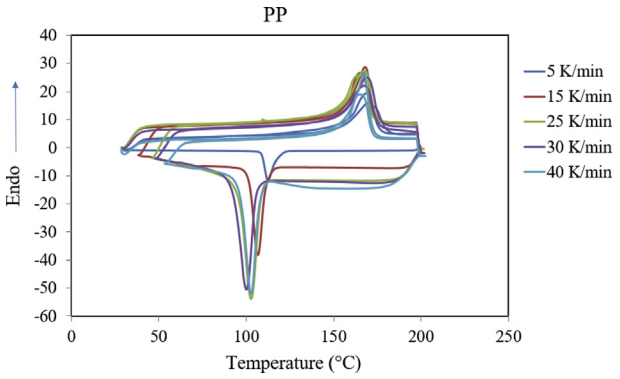

Fig. 3. DSC thermographs for PP recorded under non-isothermal conditions.

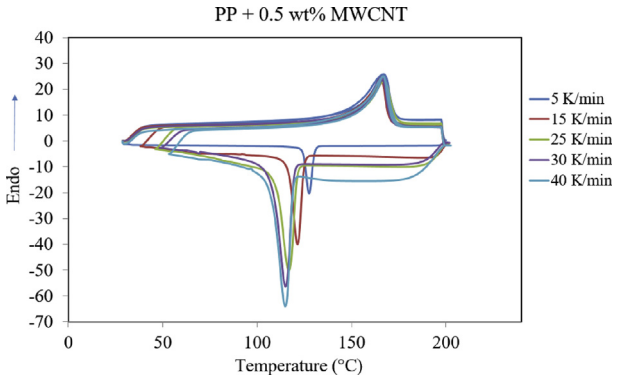

Fig. 4. DSC thermographs for the composite of PP and 0.5 wt% MWCNTs recorded under non-isothermal conditions.

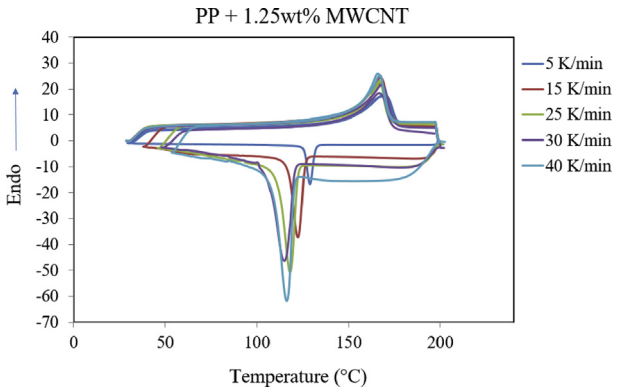

Fig. 5. DSC thermographs for the composite of PP and 1.25 wt% MWCNTs recorded under non-isothermal conditions.

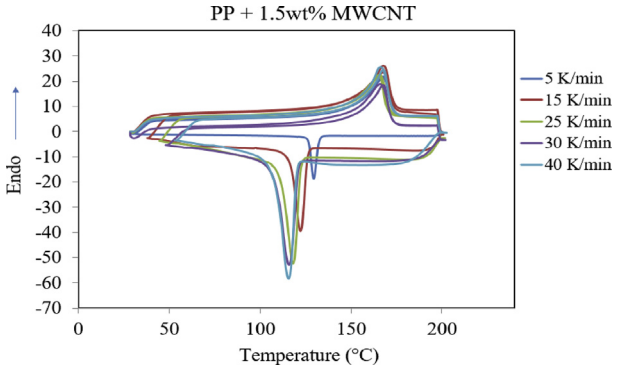

Fig. 6. DSC thermographs for the composite of PP and 1.5 wt% MWCNTs recorded under non-isothermal conditions.

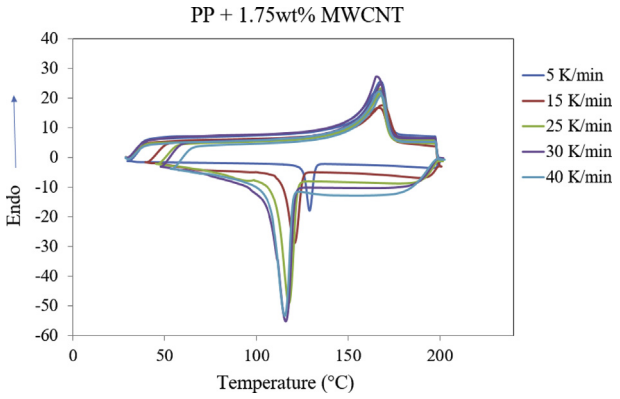

Fig. 7. DSC thermographs for the composite of PP and 1.75 wt% MWCNTs recorded under non-isothermal conditions.

3. Results & discussion

3.1. Isothermal crystallisation kinetics

As the crystallization temperature, T_c for each sample was increased, the crystallization endotherms shifted to longer time scales and became less intense leading to an increase in the total crystallization time and an increase in crystallization temperature. Using Pyris software, the values of relative crystallinity in terms of time X(t), were determined for each endotherm allowing a plot of X(t) versus time (min) to be produced. The graphs show the time taken for X(t) to equal 1, see Fig. 8. It is clear that for all samples considered, as T_c increased, the time in which crystallization occurred became progressively longer. This change is attributed to the temperature gradient between the melt and crystallization temperatures T_m and T_c, respectively. Thus for high temperature, close to the value of T_m for a given sample, there will not be a large temperature gradient, thus crystallization will occur over a longer period of time. Correspondingly, a lower temperature closer to the desired temperature of crystallization will effectively quench the sample when cooled, and thus a shorter time scale is apparent due to rapid crystallization.

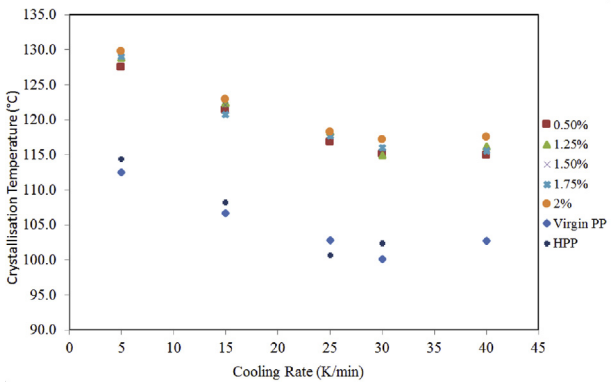

Fig. 8. Variation in crystallisation temperature with cooling rate for different CNT loadings.

As an increase in the relative degree of crystallinity is seen with an increase in crystallisation time *t*, the Avrami equation [24,27,28], can be used to analyse the isothermal crystallisation of PP and composites of PP and MWCNTs considered as a function of crystallisation time and temperature as shown by:

$$X(t) = 1 - \exp(-kt^n) \tag{1}$$

In order to determine the Avrami exponent, n and the rate parameter, k, a plot of log [−ln(1−X(t))] versus log time was produced for each sample studied, see Fig. 9. A two-stage crystallization process is evident as indicated from the linear portion of the plots and subsequent slight deviations, respectively. The values of n and K were determined from the slope and intercept of the initial linear portion of each plot and are recorded in Table 1, with values for the Avrami exponent (n) being calculated as greater than 2. This confirms that the primary stage of crystal growth is a three-dimensional phenomenon for all the samples studied. Also included in Table 1 are a number of other useful parameters used for this analysis including the half-time of crystallization $t_{1/2}$, defined as the time for crystallization to reach 50%, where:

$$t_{1/2} = (\ln 2/K)^{1/n} \tag{2}$$

It is clear that $t_{1/2}$ increases with increasing T_c for all samples considered, as is the case for all polymeric materials for a lower degree of super-cooling. The rate of crystallization, $\tau_{1/2}$, is given as the reciprocal of $t_{1/2}$. Using these values, t_{max}, the time required for maximum crystallisation rate, was determined. t_{max} is the point at

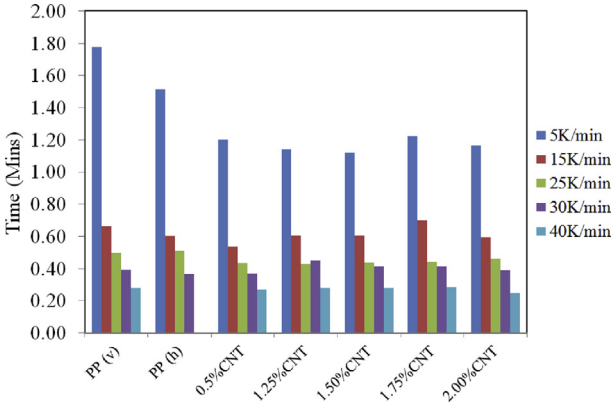

Fig. 9. Variation in crystallisation time with increasing CNT loading at different cooling rates.

which the rate of change of heat flow rate with time is equal to zero, given by:

$$t_{max} = [(n-1)/nK]^{1/n} \tag{3}$$

The values calculated for t_{max} are also listed in Table 1.

Cebe and Hong [18], reported that assuming a thermally activated crystallisation process the crystallisation rate parameter could be determined by use of an Arrhenius type equation, as follows;

$$K^{1/n} = k_0 \exp -\frac{\Delta E}{RT_C} \tag{4}$$

A plot of 1/n(ln K) versus $1/T_c$ was produced for each sample considered in order to determine ΔE, the activation energy for crystallisation (kJ), see Fig. 10. ΔE for unfilled PP was 58 kJ however, ΔE increased to 87 kJ on addition of 1.25 wt% MWCNTs but a more significant increase in ΔE to 228 kJ was determined when the MWCNT loading was increased to 2 wt%, which may be associated with attaining percolation.

3.2. Non-isothermal crystallisation

Analysis of the non-isothermal crystallization exotherms of each sample studied from the melt at any of the considered cooling rates reveals several useful parameters which can be obtained via simple inspection, interpretation and comparison of the crystallisation behaviour of the specific sample under examination. T_{cp} is defined as the crystallization peak temperature during cooling and T_c onset is the onset temperature of crystallisation. The difference between T_c onset and T_{cp} is inversely related to the general rate of crystallization. T_{mp1} and T_{mp2}, the peak melting temperatures for the first and second melting and ΔH_{m1} and ΔH_{m2}, the enthalpy of melting for the first and second melts respectfully for all samples were obtained from each DSC thermograph. X_c, the degree of crystallinity was also determined by using the equation:

$$X_c = \frac{\Delta H_m}{(1-\psi)\Delta H_{100}} \times 100 \tag{5}$$

where, (1−ψ) is the weight fraction of polymer, and ΔH_{100} is the theoretical enthalpy value for 100% crystalline poly(propylene), which is taken to be 209 J/g [5]. From each DSC trace at varying cooling rates, the thermal parameters can be determined from the exotherms and endotherms of each sample, by way of example, see Tables 2 and 3 for the parameters determined for cooling rates of 5 and 40 K/min., respectively. The values of T_c onset and T_{cp} for the composites are higher than that of unfilled PP either before, PP(v) or after PP(h) melt processing. The values of both T_c onset and T_{cp} increase with MWCNT loading under the conditions considered here, i.e. cooling rates of 5 and 40 K/min. However, this is only true up to a particular loading of MWCNTs under each condition, i.e. 1.5 wt% MWCNTs for a cooling rate of 5 K/min. and 1.25 wt% MWCNTs CNT for T_{cp} and T_c onset for a cooling rate of 40 K/min. In all cases there is a shift in both T_{cp} and T_c onset for lower CNT loadings, up to 0.5 wt%. Additional MWCNT loading results in a slight increase, (non-linear), in T_{cp} and T_c onset.

3.2.1. Heterogeneous nucleation

For the same cooling rate the crystallisation temperature, T_{cp} of the composites at any given MWCNT loading is higher than that of the unfilled polymer, as shown see Table 4 and irrespective of cooling rate, see Fig. 11. This behaviour is related to the heterogeneous nucleation of PP initiated by the MWCNTs which alters the crystallization process during cooling from a temperature above

Table 1
Parameters determined from the Avrami equation.

	n	K	$t_{1/2}$	$T_{1/2}$	t_{max}	Temp (°C)	Temp (K)	$1/T_c$	1/n (ln K)
PP	2.40	2.45	0.59	1.69	1.16	108	381	0.0026	0.37
	2.56	2.17	0.64	1.56	1.11	112	385	0.0026	0.30
	2.94	2.18	0.68	1.48	1.13	114	387	0.0026	0.27
	2.42	0.82	0.93	1.07	0.74	117	390	0.0026	−0.08
	2.85	−0.51	–	–	–	122	395	0.0025	–
1.25 wt%CNT	2.50	2.40	0.61	1.64	1.16	124	397	0.0025	0.35
	2.86	2.20	0.67	1.50	1.13	127	400	0.0025	0.27
	2.70	1.71	0.72	1.40	1.03	129	402	0.0025	0.20
	3.03	1.27	0.82	1.22	0.95	131	404	0.0025	0.08
	2.82	0.40	1.21	0.82	0.62	134	407	0.0025	−0.32
2 wt%CNT	3.41	3.25	0.64	1.57	1.28	123	396	0.0025	0.34
	2.54	2.14	0.64	1.56	1.11	127	400	0.0025	0.30
	2.99	2.09	0.69	1.45	1.12	129	402	0.0025	0.25
	2.75	1.29	0.80	1.25	0.93	131	404	0.0025	0.09
	2.79	0.01	5.68	0.18	0.13	135	408	0.0025	−1.87

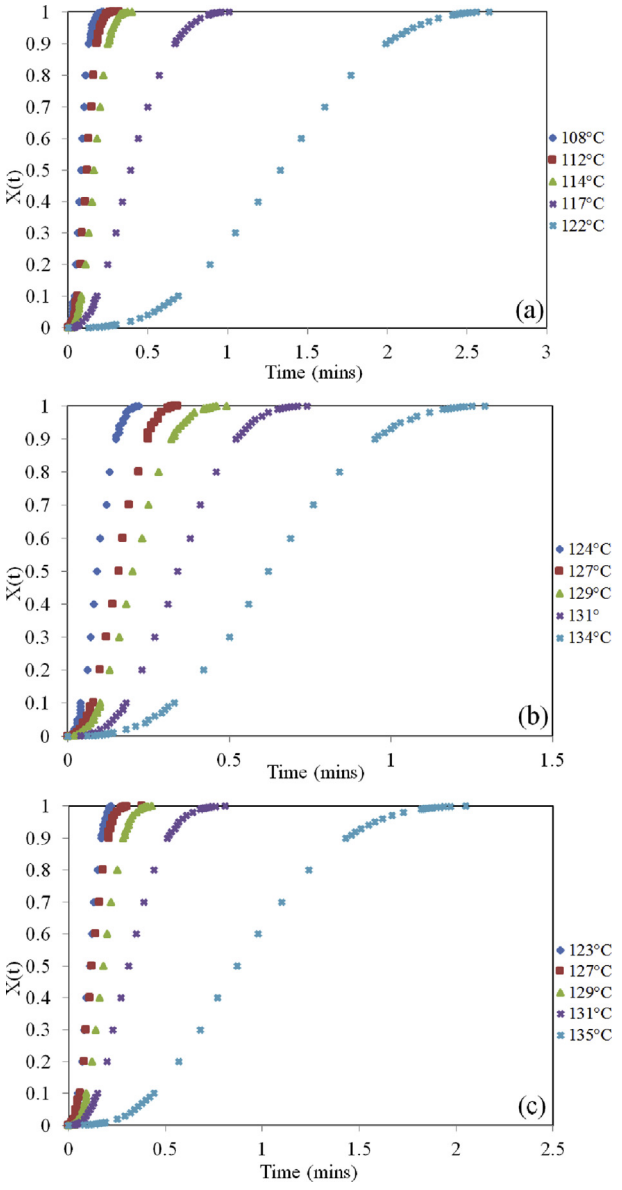

Fig. 10. X(t) versus time for isothermal crystallisation of a) neat PP and composites of PP with b) 1.25 wt% CNT and c) 2 wt% CNT.

the melting point of PP [3,27]. Nucleation occurs because the solid surfaces of the MWCNTs and other impurities within the polymer act as nuclei on which PP chains can easily be absorbed. This leads to more rapid crystallization at higher temperatures.

For a given polymer, nucleation efficiency (NE) has been defined by Fillon et al. [24] as, by way of example for the composite with a MWCNT loading of 2 wt%,

$$NE = \frac{T_{cp2\%} - T_{cpPP(v)}}{T_{cmax} - T_{cpPP(v)}} \quad (6)$$

where, $T_{cp\ PP}$ is the peak crystallization temperature of poly(-propylene) without any nucleating agent being added. $T_{cp2\%}$ is the peak crystallization temperature of the composite with 2 wt% MWCNTs added (the nucleating agent) and T_{cmax} is the optimum self-nucleation temperature which has been reported to be 164.5 °C for PP [24]. For the slowest and fastest cooling rates studied [5 and 40 K/min.], the NE for the composite of PP and 2 wt% MWCNTs was calculated as 33% and 23.8%, respectively, confirming the MWCNTs acted as a nucleating agent for PP.

To investigate the overall effect of cooling rate and MWCNT content on the overall crystallization time, T_c of each individual sample the following equation was applied,

$$T_c = \frac{T_{onset} - T_{end}}{\alpha} \quad (7)$$

where, α is equal to the cooling rate being considered. As can be seen from Fig. 12, an increase in cooling rate significantly reduces the crystallization time for all samples studied.

3.2.2. Non-isothermal mathematical modelling

To more accurately describe the non-isothermal crystallisation kinetics of the composites of PP and MWCNTs, several mathematical models which apply to polymers have been developed. Their relevance to PP as a function of MWCNT loading was investigated using the following models; 1) Jeziorny extended Avrami equation, 2) Ozawa equation, 3) Cazé Average Avrami exponent, 4) Chuah Average Avrami exponent, 5) Combined Avrami/Ozawa Equation and 6) Kissinger activation energy.

3.2.2.1. Jeziorny-modified Avrami equation. Assuming the crystallization temperature for any given sample is constant the Avrami equation can be used to describe the primary stage of the non-isothermal crystallization, as considered by Mandelkern [29]. The Jeziorny-modified Avrami equation is based on the assumption that the cooling rate remains constant or approximately constant for a

Table 2
Non-isothermal endotherm data for samples cooled at 5 K/min.

Sample	PP (v)	PP (h)	0.5 wt% CNT	1.25 wt% CNT	1.5 wt% CNT	1.75 wt% CNT	2 wt% CNT
1st heating							
$T_{m1\ onset}$ (°C)	153.6	153.1	152.7	150.2	152.7	154.4	154.3
$T_{m1\ end}$ (°C)	180.2	181.3	172.8	176.0	173.0	173.1	172.4
T_{mp1} (°C)	169.9	170.9	166.6	168.7	167.5	167.8	165.9
Area (mJ)	616.9	804.5	808.0	677.1	735.9	799.0	923.8
ΔH_{m1} (J/g)	74.3	100.6	101.0	84.6	87.6	101.1	112.7
$\%X_t$	35.5	48.1	48.51	41.0	42.5	49.2	55.0
Cooling							
$T_{c\ onset}$ (°C)	117.9	118.7	130.5	131.8	132.4	132.0	132.6
$T_{c\ end}$ (°C)	109.0	111.2	124.5	126.1	126.8	125.8	126.8
T_{cp} (°C)	112.6	114.4	127.5	128.9	129.5	129.1	129.7
Area (mJ)	−763.0	−975.6	−868.7	−730.8	−736.0	−816.4	−775.3
ΔH_c (J/g)	−91.9	−121.9	−108.6	−91.4	−89.8	−103.3	−94.5
2nd heating							
$T_{m2\ onset}$ (°C)	156.4	155.1	149.7	149.9	150.8	149.3	149.3
$T_{m2\ end}$ (°C)	175.9	172.8	172.2	176.8	173.1	172.7	172.9
T_{mp2} (°C)	168.7	165.5	167.0	169.1	167.8	166.9	166.9
Area (mJ)	753.0	931.0	926.4	710.6	786.4	832.6	831.7
ΔH_{m2} (J/g)	90.7	116.4	115.8	88.8	93.6	105.4	101.4
$\%X_t$	43.4	55.6	55.6	43.0	45.4	51.33	49.5

given sample being considered. Thus, the final form of the rate parameter characterizing the kinetics of non-isothermal crystallization can be given by:

$$\log Z_c = \log \frac{Z_t}{\lambda} \tag{8}$$

From the above equation the rate parameter Z_c or Z_t, and the Avrami exponent, n can both be determined from the intercept and slope of a plot of $\log[-\ln(1-X(t))]$ versus log time, see Fig. 13. From the change in the slope, a two-stage crystallization process is evident and with values of n, Z_c and Z_t determined and listed in Table 5. During the initial primary stages of crystallization the Avrami exponent, n_1 varies from approximately 3.30 to 4.27 for the composite of PP and 2 wt% MWCNTs and from 2.91 to 3.60 for the neat PP indicating a complex crystallization process at the primary stage for both materials. Again, the effect of MWCNT addition to PP can be observed, irrespective of cooling rate, on the overall crystallization process. A maximum value of $n_1 = 4.518$ was determined for 2 wt% MWCNT composite in comparison to $n_1 = 3.595$ for unfilled PP. Z values for both minimum and maximum MWCNT loadings increase with increasing cooling rate indicating faster crystallization, with larger values obtained for MWCNT filled PP. As the Avrami exponent was greater than 2 for all blends studied the primary crystallization stage can be described as a three-dimensional growth phenomenon as proposed by Wunderlich [30]. In comparison to the values of n_1, those of n_2 decreased considerably due to spherulite impingement in the latter stages of crystallization Therefore, assigning an average value of n was difficult using this model. However, Ozawa described a method specifically designed to model non-isothermal crystallization kinetics [21].

3.2.2.2. Ozawa analysis. Ozawa extended the Avrami equation to allow for all the processes of non-isothermal crystallisation. A graph of $\ln[-\ln(1-X(t))]$ versus $\log \lambda$ was plotted from data points taken at different temperatures in the range 369 K–389 K for PP at 1 K intervals and in the range of 392 K–399.5 K in 0.5 K intervals for the composite of PP and 2 wt% MWCNTs. By modelling the crystallization behaviour of PET, Ozawa reported his analysis showed good agreement by plotting a series of parallel straight lines constructed across a range of crystallization temperatures,

Table 3
Non-isothermal endotherm data for samples cooled at 40 K/min.

Sample	PP (v)	PP (h)	0.5 wt% CNT	1.25 wt% CNT	1.50 wt% CNT	1.75 wt% CNT	2 wt% CNT
1st heating							
$T_{m1\ onset}$ (°C)	156.4	153.1	153.2	155.8	156.3	154.0	156.2
$T_{m1\ end}$ (°C)	172.1	181.3	172.6	172.2	172.7	173.0	171.8
T_{mp1} (°C)	167.6	170.9	166.8	166.0	166.6	166.9	167.2
Area (mJ)	786.9	804.5	888.6	749.6	815.5	734.5	733.1
ΔH_{m1} (J/g)	102.2	100.6	104.5	97.3	98.3	95.4	91.6
$\%X_t$	48.9	48.1	50.3	47.1	47.7	46.5	44.7
Cooling							
$T_{c\ onset}$ (°C)	108.0	119.1	119.1	120.4	120.2	119.8	121.3
$T_{c\ end}$ (°C)	96.8	111.2	108.3	109.2	108.9	108.5	111.4
T_{cp} (°C)	102.8	114.4	114.9	116.2	115.6	115.5	117.5
Area (mJ)	−739.6	−810.2	−810.2	−784.2	−820.8	−708.5	−765.6
ΔH_c (J/g)	−96.0	−95.3	−95.3	−101.8	−98.9	−92.0	−95.7
2nd heating							
$T_{m2\ onset}$ (°C)	155.8	155.1	157.8	156.6	157.0	156.2	157.9
$T_{m2\ end}$ (°C)	171.8	172.8	171.1	171.3	172.2	172.9	170.4
T_{mp2} (°C)	165.4	165.5	166.8	167.1	167.8	168.1	166.8
Area (mJ)	590.8	931.0	689.7	710.4	667.5	657.9	677.1
ΔH_{m2} (J/g)	76.7	116.4	81.1	92.3	80.4	85.4	84.6
$\%X_t$	36.7	55.7	38.9	44.7	39.1	41.6	41.3

Table 4
Crystallisation temperatures for all samples in the non-isothermal study.

Cooling Rate (K/min)	Crystallisation Temperature (°C)						
	Virgin PP	HPP	0.5 wt%CNT	1.25 wt%CNT	1.5 wt%CNT	1.75 wt%CNT	2 wt%CNT
5	112.6	114.4	127.5	128.9	129.5	129.1	129.7
15	106.7	108.2	121.4	122.4	122.2	120.8	122.9
25	102.9	100.7	116.9	118.2	118.1	117.7	118.3
30	100.1	102.3	115.1	114.9	115.9	116.1	117.2
40	102.8	–	114.9	116.2	115.6	115.5	117.5

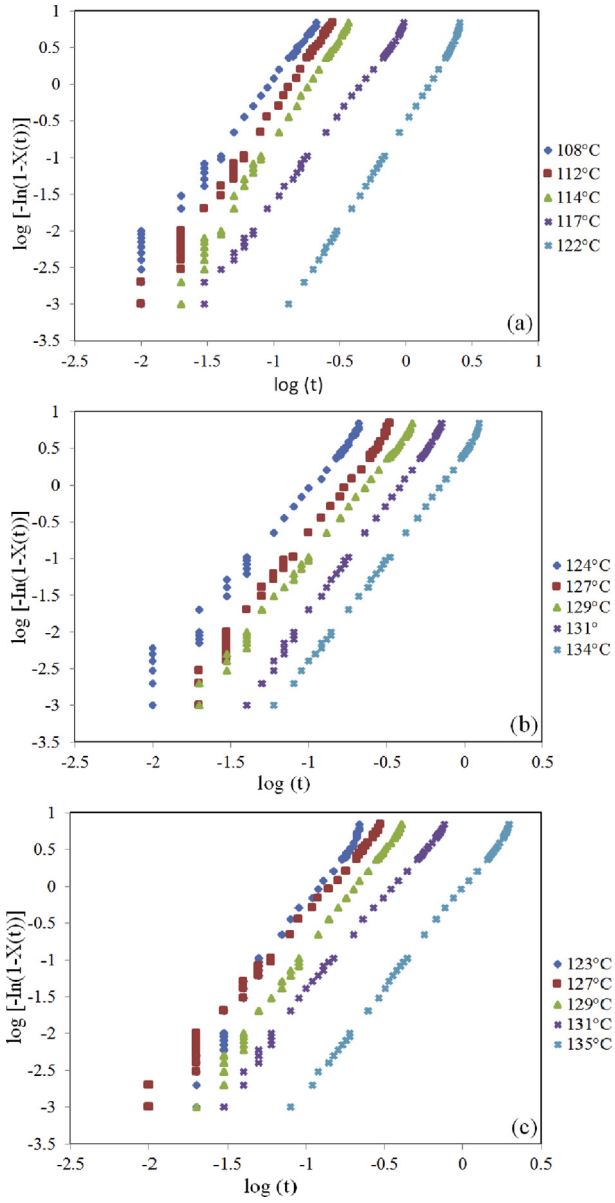

Fig. 11. Avrami plot for the isothermal crystallisation of a) neat PP and composites of PP with b) 1.25 wt% MWCNTs and c) 2 wt% MWCNTs.

$$1 - X_t = \exp\left[-\frac{K(T)}{\Phi^m}\right] \tag{9}$$

where, K(T) is the cooling or heating function, Φ is the cooling or heat rate and m is the Ozawa exponent that depends on the dimensionality of crystal growth. However, as seen in Fig. 14 this model is limited for higher cooling rates. For this model to work the

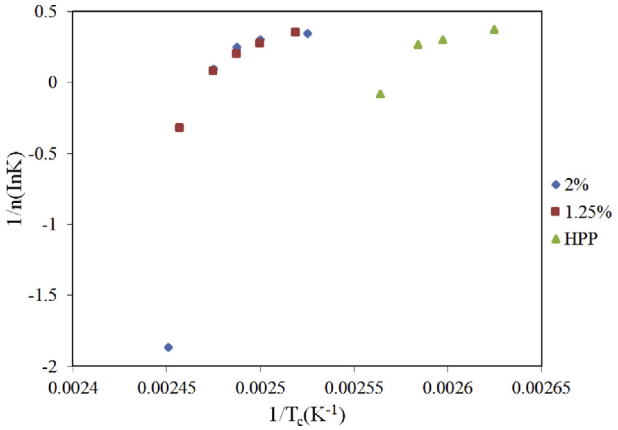

Fig. 12. Plot of 1/n(lnK) versus 1/Tc for the Avrami parameter K obtained from isothermal crystallisation data.

40 K/min. cooling rate was excluded from all calculations, the remaining data listed in Table 6. By applying the Ozawa model to the results obtained, a clear two-stage crystallization process is evident. However, the changing slope with temperature indicates that m is not constant during crystallization and therefore the Ozawa model cannot accurately describe non-isothermal crystallization of composites of PP loaded with MWCNTs. This observation suggests the possibility of a three-stage crystallization process for these materials.

3.2.2.3. Cazé average Avrami exponent. Based on the three temperature inflection points, $T_{c\ onset}$, T_c and $T_{c\ end}$ obtained from the DSC cooling curves, an average value for the Avrami exponent, n can be determined as reported by Cazé [19]. With this approach the three temperatures vary linearly with cooling rate. A plot of inflection temperature versus ln cooling rate was produced, Fig. 15 and, again neglecting the data for a cooling rate of 40 K/min. there is good agreement between the results obtained and that predicted by the Cazé model. From the experimental results obtained the coefficients A, B_1 and B_2 were calculated, A = −6.40 and 6.13, B_1 = 128.49 and 142.69, and B_2 = 122.78 and 142.45, for unfilled PP and the composite of PP with 2 wt% MWCNTs, respectively. Using these values, n can be calculated from:

$$T_i = A \ln \lambda + B_i \tag{10}$$

where, A and B are calculated from the slope and intercept of the linear plots, respectively.

$$n = A\frac{\ln\left(\frac{3-\sqrt{5}}{3+\sqrt{5}}\right)}{B_1 - B_2} \tag{11}$$

Thus n was determined to be 2.16 and 49.18 for unfilled PP and the 2 wt% MWCNT composite, respectively, values different from those determined using the Jeziorny method.

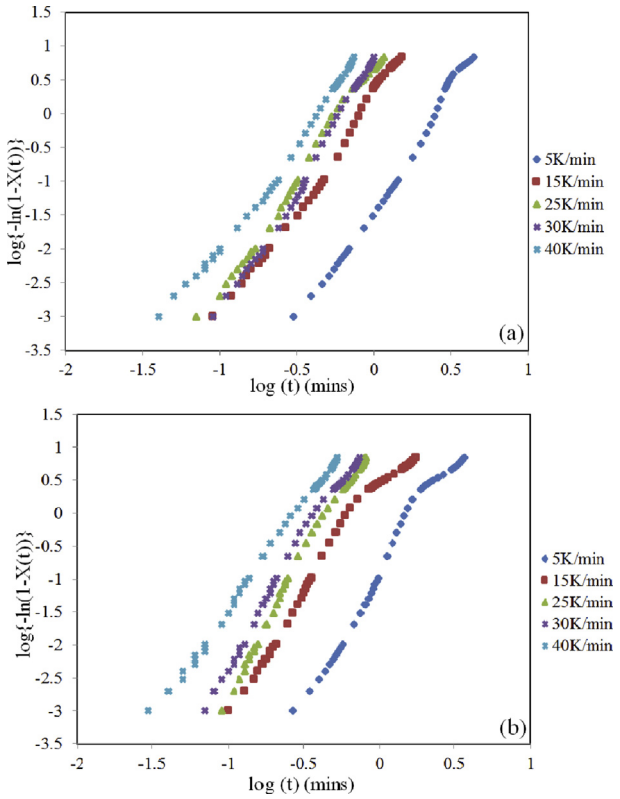

Fig. 13. Jeziorny plot of log{−ln(1−X(t))} versus log time for a) neat PP and b) a composite of PP with 2 wt% MWCNTs.

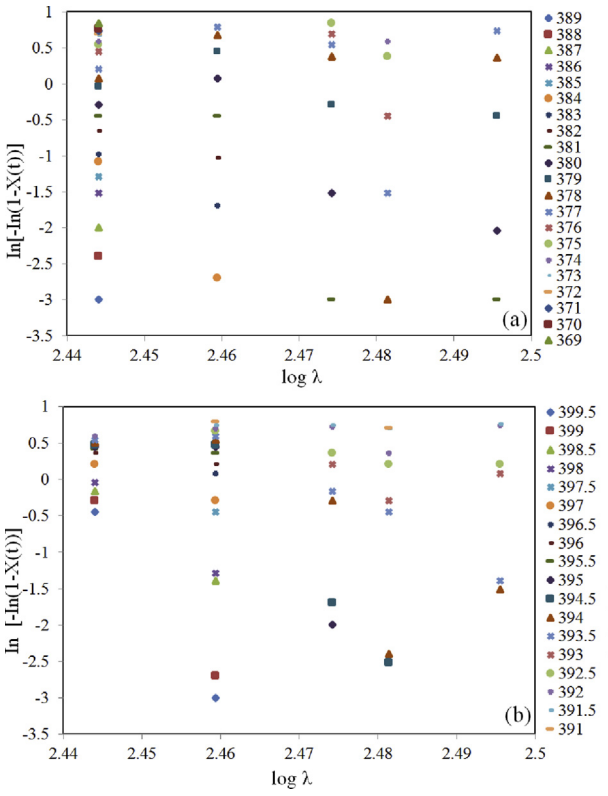

Fig. 14. Ozawa plot of ln[−ln(1−X(T))] versus log λ for a) neat PP and b) a composite of PP and 2 wt% CNT.

3.2.2.4. Chuah method for average Avrami exponent. Based on the Ozawa equation, Chuah reported that the following method may be used to account for shortcomings in both the Ozawa and Cazé methods. From the DSC endotherms the weight fraction and volume fraction, X_v of the crystal structure were calculated using,

$$X_v T = \frac{X_w T \frac{\rho_a}{\rho_c}}{1 - \left[1 - \frac{\rho_a}{\rho_c}\right] X_w T} \tag{12}$$

Accounting for the temperature effects on the ratio ρ_a/ρ_c the empirical rules reported by Boyer- Spencer-Bondi, the values of the glass transition temperature and equilibrium melting temperature were taken as 256.2 and 444.2 K as reported by Chuah [17]. The following equation was then used to evaluate the ratio of ρ_a/ρ_c (i.e. the densities of the amorphous and crystalline phases of PP) for PP,

$$\frac{\rho_a}{\rho_c} = \left(\frac{\rho_{ao}}{\rho_{co}}\right) \exp\left[(T - T_r)\left(\frac{0.11}{T_m^o} - \frac{0.16}{T_g}\right)\right] \tag{13}$$

where, 'o' refers to properties at the reference temperature, the values of ρ_{ao} and ρ_{co} were reported by Chuah as 0.85 and 0.936 respectively and, T_r was taken as 298 K. From this, Chuah proposed that the primary crystallization stage for a given polymer could be determined using two equations;

$$\ln K^* T = \alpha(T - T_1) \tag{14}$$

$$K^* T_\lambda = \lambda^n \tag{15}$$

Using this approach a plot of ln[−ln(1−X_v)] versus T was produced, whereby the constants, α (coefficient of thermal expansion) and αT_λ were determined from the gradient and intercept of plots respectively, see Fig. 16 and the relevant parameters listed in

Table 5
Values of exponents from the Jeziorny-Modified Avrami equation for the two-stage non-isothermal crystallization of neat PP and a composite of PP and 2 wt% MWCNTs.

λ (K/min)	log λ	n_1	n_2	Z_{c1}	Z_{c2}	log Z_{c1}	log Z_{c2}	log Z_{t1}	log Z_{t2}
PP									
5	0.698	3.595	1.741	−0.297	−1.392	–	–	–	–
15	1.176	3.157	2.475	0.393	0.142	−0.404	−0.845	−6.072	−12.687
25	1.397	3.559	2.190	0.667	0.830	−0.175	−0.080	−4.381	−2.015
30	1.477	3.752	3.378	0.798	0.749	−0.097	−0.125	−2.936	−3.761
40	1.602	2.912	3.341	1.240	0.939	0.093	−0.027	3.737	−1.087
2 wt% MWCNTs									
5	0.698	4.265	1.487	−0.887	−0.042	–	–	–	–
15	1.176	4.005	1.403	0.798	0.453	−0.097	−0.343	−1.462	−5.145
25	1.397	4.518	3.001	1.679	1.066	0.225	0.027	5.631	0.699
30	1.477	4.165	2.597	1.793	1.125	0.253	0.051	7.614	1.541
40	1.602	3.303	2.911	1.847	1.607	0.266	0.206	10.664	8.249

Table 6
Ozawa parameters for the two-stage non-isothermal crystallisation of neat PP and a composite of PP and 2 wt% MWCNTs.

Temp. (K)	m_1	m_2	lnK(T)1	lnK(T)2
PP				
384	−105.5	–	256.8	–
383	−46.7	–	113.2	–
382	−24.4	–	58.9	–
381	0.0	−172.2	−0.4	423.0
380	24.3	−107.7	−59.6	265.0
379	31.7	−50.0	−77.6	123.4
378	38.6	−144.7	−94.3	357.1
377	38.2	−91.7	−93.2	226.5
376	–	−158.2	–	392.2
375	9.8	−63.3	−23.3	157.5
2 wt% MWCNT				
399.5	−166.3	–	406.0	–
399	−156.8	–	383.0	–
398.5	−80.1	–	195.7	–
398	−81.6	–	199.3	–
397.5		–		–
397	−32.5	–	79.6	–
396.5	−80.1	–	195.7	–
396	−10.1	–	25.1	–
395.5	−4.1	–	10.4	–
395	0.0	−165.1	0.4	406.4
394.5	0.0	−137.6	0.5	338.7
394	2.4	−122.0	−5.4	300.8
393.5	3.1	−47.7	−7.0	117.9
393	–	−69.0	–	−65.8
392.5	–	−20.6	–	51.4
392	6.7	−12.6	−15.8	31.7
391.5	–	−1.8	–	5.2
391	−156.8	–	383.0	–

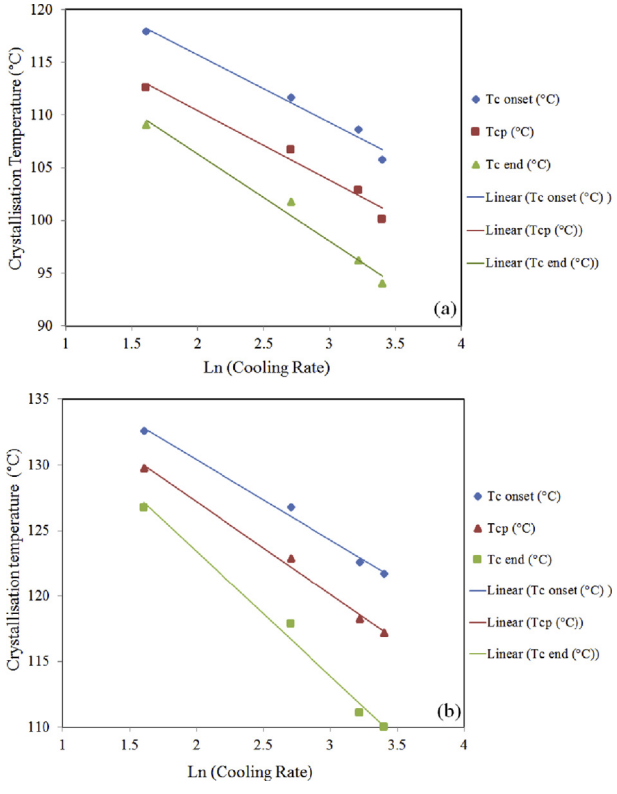

Fig. 15. Evolution of T_c onset, T_c and T_c end for a) PP and b) a composite of PP and 2 wt% MWCNTs.

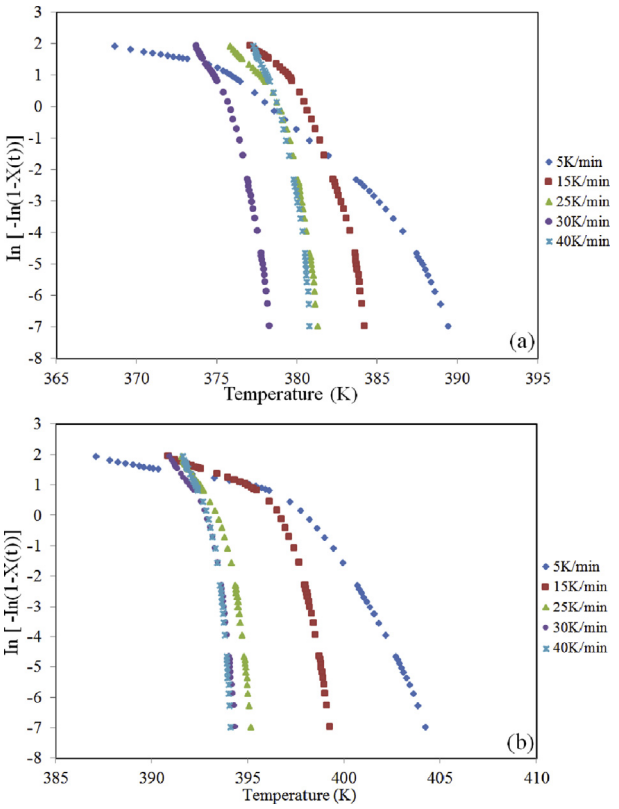

Fig. 16. Chuah plot of $\ln[-\ln(1-X_v)]$ versus temperature for a) neat PP and b) a composite of 2 wt% MWCNTs at different cooling rates.

Table 7. It is clear that a two stage crystallization process exists for both unfilled PP and the composites of PP and MWCNTs. From a plot of ln λ/α versus T_λ for all cooling rates n was determined from the slope of the linear portion of the curves. Table 7 displays the data used to construct this plot. The values for n calculated from the linear plots (Fig. 17 and Table 8) vary considerably from those determined from the previous models. Therefore, further investigation is needed in order to determine the reason for the difference.

3.2.2.5. Combined Avrami and Ozawa equation. In effect, the models discussed above only effectively describe the primary stage of crystallization and do not account for any subsequent stages. To completely describe the non-isothermal crystallization process of the various samples Mo et al. proposed another model for non-isothermal crystallization based on combining the Avrami and Ozawa equations [31,32],

$$\log \Phi = \log F(T) - \alpha \log t \tag{16}$$

where, $F(T) = [K(T)/Z_t]^{1/m}$ and $\alpha = n/m$, the ratio of the Avrami to Ozawa exponents. For a given value of X_t a plot of log cooling rate versus log time was produced at several X_t values ranging from 20% to 90% in 10% intervals, Fig. 18. It can be seen these plots yield a series of linear relationships for each material studied for a given X_t thereby showing the Mo model can successfully describe the non-isothermal crystallization of PP and composites of PP and MWCNTs. For a given value of X_t, the values of α and F(T) were determined from the slope and intercept of the best-fit trend line drawn through the data points for each cooling rate considered at the assigned value of X_t, Table 9. The values of F(T) increase systematically with increasing crystallinity as reported by Liu et al. [20], indicating that in order to obtain a higher degree of crystallinity a

Table 7
Chuah parameters used for calculation of an average Avrami exponent from plots of T_λ vs ln λ/α.

Cooling rate (K/min)	α	αT_λ	T_λ	$\ln\lambda/\alpha$
PP				
5	−0.47	187.32	−394.52	−3.39
15	−0.93	365.38	−394.67	−2.93
25	−2.11	827.15	−392.82	−1.53
30	−2.24	879.63	−392.23	−1.52
40	−3.03	1190.26	−392.52	−1.22
2 wt% MWCNT				
5	−0.42	159.44	−376.88	−3.80
15	−1.17	446.04	−379.83	−2.31
25	−1.47	553.98	−377.96	−2.20
30	−1.74	654.73	−375.25	−1.95
40	−2.21	837.43	−378.46	−1.67

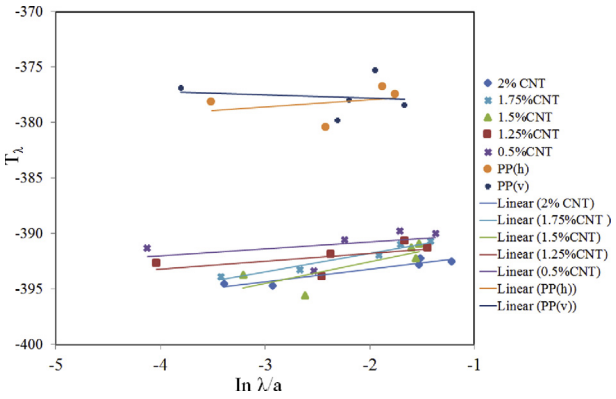

Fig. 17. Chuah plot of T_λ versus ln λ/a for neat PP and composite of PP with MWCNTs.

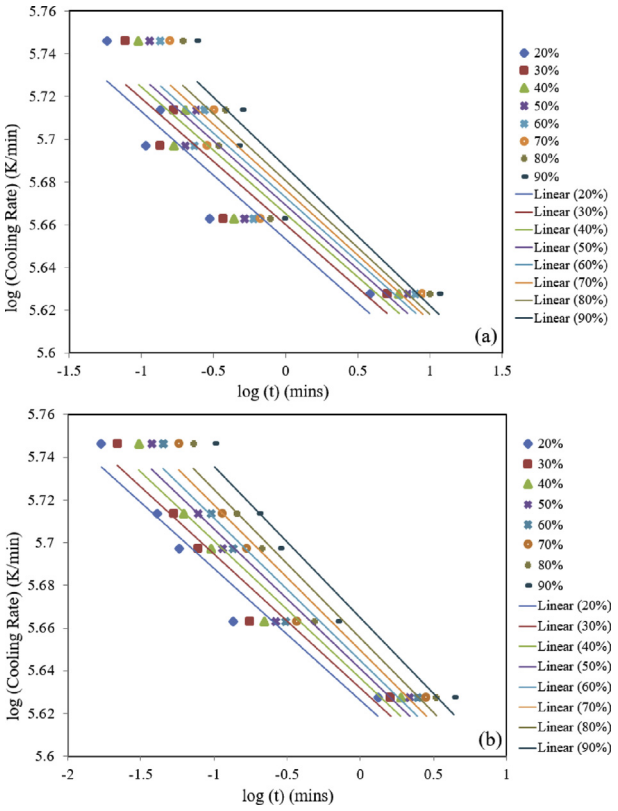

Fig. 18. Combined Avrami and Ozawa plots for a) PP and b) a composite of PP and 2 wt % MWCNTs at various degrees of crystallisation.

higher cooling rate should be used. Mo stated that the values of α remained almost constant [33], regardless of X_t, this is in agreement with the data presented in Table 9. From Fig. 18 the typical slower cooling rate results in a longer time over which crystallisation occurs and vice versa. Additionally, higher cooling rates widen the spread of log t, which then narrows as the cooling rate is reduced, causing an increase in the value of α. Therefore, α can be considered to be strongly cooling rate dependent.

A linear equation of the form $b = AX_t + C$ was found to fit with the data plotted in Fig. 19(a), supporting the conclusion that b is strongly cooling rate dependent. From the slope and intercept A and C for unfilled PP were found to be −0.0001 and −0.0589, while A and C for the composite of PP and 2 wt% MWCNTs were found to be −0.00007 and −0.057. A linear relationship was also found from Fig. 19(b) of the form $\log F(T) = DX_t + E$ where, D and E are found from the slope and intercept of the plots respectively and have values of −0.00004 and 0.7494 for unfilled PP and 0.00003 and 0.7517 for the composite of PP and 2 wt% MWCNTs.

3.2.2.6. Kissinger activation energy (ΔE). Kissinger reported the activation energy for non-isothermal crystallization could be determined based on the following equation, accounting for the influence of varying cooling rates,

$$k_T = A^{\frac{-E}{RT}} \quad (17)$$

Table 9
Values of α and F(T) as a function of X(t) for PP and a composite of PP and 2 wt% MWCNTs.

X(t)	α	F(T)	Log F(T)
PP			
20	−0.06	5.65	0.75
30	−0.06	5.66	0.75
40	−0.06	5.67	0.75
50	−0.06	5.67	0.75
60	−0.06	5.67	0.75
70	−0.06	5.68	0.75
80	−0.06	5.68	0.75
90	−0.06	5.69	0.75
2 wt% MWCNT			
20	−0.06	5.63	0.75
30	−0.06	5.63	0.75
40	−0.06	5.64	0.75
50	−0.07	5.64	0.75
60	−0.07	5.64	0.75
70	−0.07	5.65	0.75
80	−0.07	5.66	0.75
90	−0.07	5.66	0.75

As the maximum value of the reaction rate during crystallization occurs at T_c, the derivative at this point with respect to time is zero. Therefore, Kissinger determined the activation energy, ΔE, using the following equation:

Table 8
Values of n determined using the Chuah method.

Blend	PP (v)	PP (h)	0.5 wt%CNT	1.25 wt%CNT	1.5 wt%CNT	1.75 wt%CNT	2 wt%CNT
n value	−0.3082	0.630672	0.626531	0.694685	1.931721	1.662612	1.13113

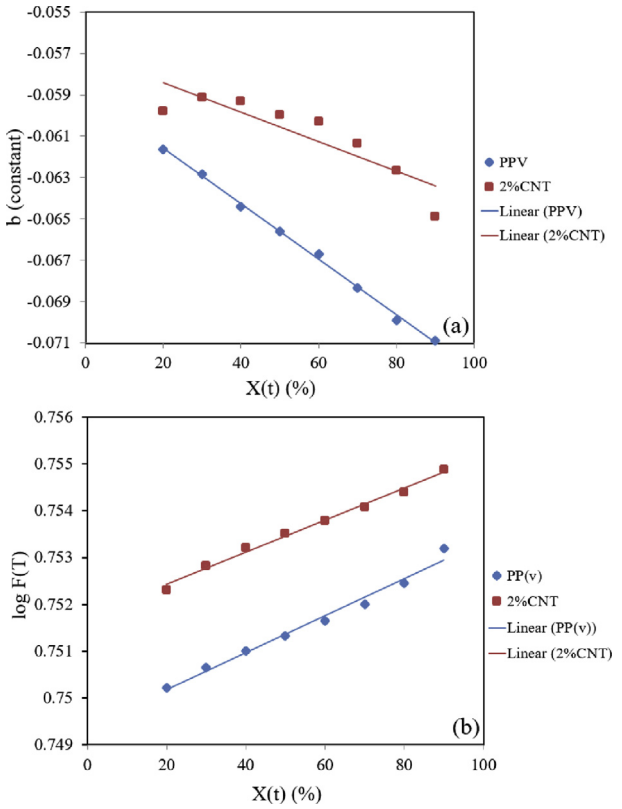

Fig. 19. Plots of a) exponent b versus X(t) and b) of log F(T) vs X(t) for combined Avrami/Ozawa treatment.

$$A^{\frac{-E}{RT_c}} = \frac{E}{RT_m^2}\frac{dT}{dt} \tag{18}$$

The above can then be written as,

$$\frac{d\left[\ln\left(\frac{\lambda}{T_c^2}\right)\right]}{d\left(\frac{1}{T_c}\right)} = -\frac{\Delta E}{R} \tag{19}$$

where, $dT/t = \lambda$ is the cooling rate, ΔE is the activation energy for crystallization and R is the universal gas constant. Fig. 20 shows the plots of $\ln \lambda/T_c^2$ versus $1/T_c$ for each sample studied from which $\Delta E/R$

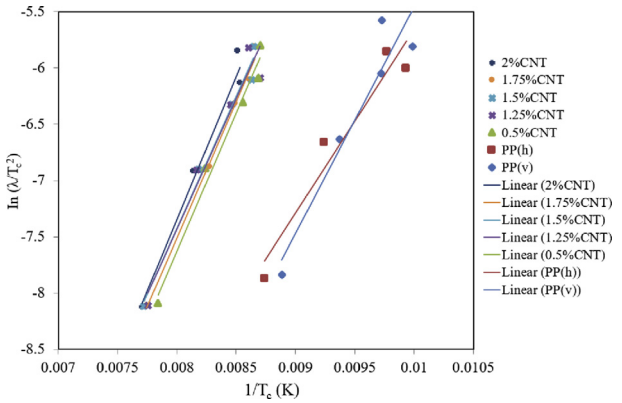

Fig. 20. Plot of $\ln \lambda/T_c^2$ versus $1/Tc$ (activation energy determined from Kissinger method) for neat PP and composites of PP and MWCNTs.

Table 10
Values for activation energy for neat PP and composites of PP and MWCNTs.

Sample	ΔE/R	ΔE (kJ)
PP(v)	2015	578
PP(h)	1635	469
0.5 wt% MWCNT	2450	703
1.25 wt% MWCNT	2322	666
1.5 wt% MWCNT	2340	672
1.75 wt% MWCNT	2435	699
2%wt MWCNT	2531	726

was determined from the slope of the best fit trend line of each plot and Table 10 lists the corresponding ΔE values. It is apparent that the addition of MWCNTs to PP results in an increase in ΔE. This phenomenon has also been reported for PP nucleated with sodium benzoate [7], rosin-based nucleating agents [10], and even poly(-trimethyleneterephthalate) (PTT)/clay [34] and polyethylene (PE)/clay nanocomposites [35]. The higher ΔE values for PP on addition of MWCNTs to PP makes the transportation of PP chain segments to the growing crystal surface more difficult. It has also been reported that addition of SWCNTs increased the viscosity of PP thus depressing the rearrangement of PP molecular chains [35]. Larger values for ΔE were determined for all composites of PP and MWCNTs compared to unfilled PP, Table 10.

4. Conclusions

The addition of different weight fractions of MWCNTs to PP had a profound effect on the overall crystallization kinetics of PP. From non-isothermal DSC experiments the crystallisation temperature, T_{cp} of PP shifted to higher temperatures. Increasing the MWCNT loading resulted in an increase in the crystallization temperature of PP. However, at higher loadings the dispersion and distribution of the MWCNTs if the PP becomes more difficult, the effective surface area for nucleation of PP is reduced and the degree of crystallization decreases. The Avrami exponent, n was found to be in the range 2.4–2.94, 2.5 to 3.03 and 2.99 to 3.41, for unfilled PP, and composites of PP with 1.25 wt% and 2 wt% MWCNTs, respectively. The values for activation energy for isothermal crystallization increased from 58 kJ for unfilled PP, to 87 kJ and then up to 228 kJ for a composite of PP with 2 wt% MWCNTs.

From the Jeziorny modified Avrami model, the non-isothermal crystallization kinetics of the composites is clearly a two-stage process. The value of n_1 was in the range of 0.6–1.6 and for n_2 2.9 to 3.8 and 4.1 to 4.8 for the minimum and maximum MWCNT loadings. The change in n_1 and n_2 was associated with spherulitic impingement and crowding. An attempt at fitting the Ozawa model was not successful as two different values of m (Ozawa exponent) were obtained whereas, Ozawa reported that for the equation to be valid only one value of m should exist. Using the Cazé method, exponent values of 2.16 and 49.18 were determined for PP and the 2 wt% MWCNT composite and as such this approach is deemed ineffective as it does not take into account the effect of secondary crystallization.

A combined Avrami/Ozawa plot successfully modelled the two-stage crystallization of the composites of PP and MWCNTs. The values of exponents α and F(T) were found to be strongly rate dependent. The activation energy (ΔE) for the non-isothermal crystallization of PP and PP on addition of MWCNTs was calculated to be in the range 578 kJ–726 kJ with stepped increases in ΔE with increasing weight fraction of MWCNTs.

Conflict of interest

There is no conflict of interest.

Acknowledgements

The authors thank Nanocyl S.A. for providing the MWCNTs.

References

[1] A.B. Kaganj, A.M. Rashidi, R. Arasteh, S. Taghipoor, J. Exp. Nanosci. 4 (2009) 21–34.
[2] D. Bikiaris, Materials 3 (2010) 2884–2946.
[3] T. McNally, P. Pötschke, P. Halley, M. Murphy, D. Martin, S.E.J. Bell, G.P. Brennan, D. Bein, P. Lemoine, J.P. Quinn, Polymer 46 (2005) 8222–8232.
[4] M.K. Seo, J.R. Lee, S.J. Park, Mater. Sci. Eng. A 404 (2005) 79–84.
[5] A.L. Marinelli, R.E.S. Bretas, J. Appl. Polym. Sci. 87 (2003) 916–930.
[6] J. Li, C.X. Zhou, G. Wang, Y. Tao, Q. Liu, Y. Li, Polym. Test. 21 (2002) 583–589.
[7] G.S. Jang, W.J. Cho, C.S. Ha, J. Polym. Sci. Part B: Polym. Phys. 39 (2001) 1001–1016.
[8] M. Razavi-Nouri, J. Appl. Polym. Sci. 124 (2012) 2541–2549.
[9] E. Assouline, A. Lustiger, A.H. Barber, C.A. Cooper, E. Klein, E. Wachtel, H.D. Wagner, J. Polym. Sci. Part B: Polym. Phys. 41 (2003) 520–527.
[10] J.B. Wang, Q. Dou, J. Macromol. Sci. B. 46 (2007) 987–1001.
[11] J.E.K. Schawe, P. Potschke, I. Alig, Polymer 116 (2017) 160–172.
[12] Z.I. Lin, C.W. Lou, Y.J. Pan, C.T. Hsieh, C.L. Huang, C.K. Chen, J.H. Lin, J. Compos. Mater. 52 (2018) 503–517.
[13] P. Verma, V. Choudhary, J. Appl. Polym. Sci. 132 (2015) 1–13.
[14] S. Parija, A.R. Bhattacharyya, Polym. Eng. Sci. 57 (2017) 183–196.
[15] J. Banerjee, S. Parija, A.S. Panwar, K. Mukhopadhyay, A.K. Saxena, A.R. Bhattacharyya, Polym. Eng. Sci. 57 (2017) 1136–1146.
[16] X. Ji, J.B. Chen, G.J. Zhong, Z.M. Li, J. Lei, J. Thermoplast. Compos. Mater. 29 (2016) 1352–1368.
[17] K.P. Chuah, S.N. Gan, K.K. Chee, Polymer 40 (1999) 253–259.
[18] P. Cebe, S.-D. Hong, Polymer 27 (1986) 1183–1192.
[19] C. Caze, E. Devaux, A. Crespy, J.P. Cavrot, Polymer 38 (1997) 497–502.
[20] S.Y. Liu, Y.N. Yu, Y. Cui, H.F. Zhang, Z.S. Mo, J. Appl. Polym. Sci. 70 (1998) 2371–2380.
[21] T. Ozawa, Polymer 12 (1971) 150–158.
[22] L. Valentini, J. Biagiotti, J.M. Kenny, M.A.L. Manchado, J. Appl. Polym. Sci. 89 (2003) 2657–2663.
[23] Q.J. Duan, B.A. Wang, B.D. Hong, H.P. Wang, J. Macromol. Sci. B. 49 (2010) 1094–1104.
[24] B. Fillon, B. Lotz, A. Thierry, J.C. Wittmann, J. Polym. Sci. Part B: Polym. Phys. 31 (1993) 1395–1405.
[25] T. Liu, Z. Mo, H. Zhang, J. Appl. Polym. Sci. 67 (1998) 815–821.
[26] A. Jeziorny, Polymer 19 (1978) 1142–1144.
[27] H. Zhang, Z. Zhang, Eur. Polym. J. 43 (2007) 3197–3207.
[28] N.L.A. McFerran, C.G. Armstrong, T. McNally, J. Appl. Polym. Sci. 110 (2008) 1043–1058.
[29] L. Mandlekern, Crystallization of Polymers, McGraw-Hill, New York, 1964.
[30] B. Wunderlich, Macromolecular Physics, vol. 3, Academic Press, New York, 1976.
[31] Y. An, L. Dong, Z. Mo, T. Liu, Z. Feng, J. Polym. Sci. Part B Polym. Phys. 36 (1998) 1305–1312.
[32] T. Liu, Z. Mo, S. Wang, H. Zhang, Polym. Eng. Sci. 37 (1997) 568–575.
[33] Z. Mo, Polym. Eng. Sci. 27 (1997), 568-.
[34] X. Hu, A.J. Lesser, Macromol. Chem. Phys. 205 (2004) 574–580.
[35] Q. Yuan, S. Awate, R.D.K. Misra, J. Appl. Polym. Sci. 102 (2006) 3809–3818.